



UNSTEADY FREE CONVECTIVE FLOW PAST A MOVING VERTICAL CYLINDER WITH CONSTANT TEMPERATURE

R. K. Deka and A. Paul*

Department of Mathematics, Gauhati University, Guwahati-781014 (India)

**Email: ashpaul85@gmail.com*

(Received on: 24-05-11; Accepted on: 07-06-11)

ABSTRACT

An analysis is made for transient free convective flow about an infinite moving vertical circular cylinder with constant temperature. The governing boundary layer equations are first converted into a non-dimensional form. The exact solutions of the dimensionless governing linear boundary layer equations are obtained by Laplace transform technique. Graphical results for the velocity profile, temperature profile, skin friction, Nusselt number are discussed for various physical parametric values viz. Grashof number, Prandtl number and time.

Keywords: Heat transfer, Free convection, Moving vertical cylinder, Laplace transformation,

2000 Mathematics Subject Classification: 76R10, 80A20.

1. INTRODUCTION:

The problem of free convective flow about moving vertical cylinder has wide range of application in engineering and geophysics such as nuclear reactor cooling system and underground energy transport and hence attracted the attention of many researchers. Many researchers under different physical conditions have investigated steady and unsteady free convective flow along vertical cylinders.

Sparrow and Gregg [15] first studied the heat transfer from vertical cylinders. Goldstein and Briggs [11] presented an analysis of the transient free convective flow past vertical flat plate and circular cylinder to a surrounding initially quiescent fluid by employing Laplace transform technique. The transient is initiated by a change in wall temperature of the plate or cylinder. Nagendra et al. [12] presented a boundary layer analysis of free convection heat transfer from a vertical cylinder with uniform heat flux at its surface. Gebhart & Pera [10] analysed the steady combined buoyancy effects of thermal and mass diffusion on vertical natural convection flows. Bottemanne [1] studied the combined effect of heat and mass transfer in the steady laminar boundary layer of a vertical cylinder placed in still air.

Ganesan and Rani [6] presented a numerical solution for the transient natural convection flow over a vertical cylinder under the combined buoyancy effects of heat and mass transfer by employing an implicit finite-difference method. Ganesan and Loganathan [7, 8] presented numerical solution of unsteady natural convection flow past a semi-infinite moving vertical cylinder with heat and mass transfer subjected to constant temperature and constant heat flux. Again, Ganesan and Loganathan [9] presented a numerical study of free convective flow of a viscous incompressible fluid past a moving, semi-infinite vertical cylinder with constant temperature and mass diffusion in a thermally stratified fluid medium. Elgazery and Hassan [5] presented a numerical study of radiation effect on MHD transient mixed convection flow over a moving vertical cylinder with constant heat flux through a porous medium. Recently Reddy and Reddy [13, 14] presented a numerical study of the interaction of radiation and mass transfer effects on unsteady MHD free convection flow past a semi-infinite moving vertical cylinder by employing finite-difference scheme of Crank-Nicolson type.

However, the flow past a moving vertical cylinder plays an important role in many industrial applications. Analytical study of unsteady free convective flow over a vertical cylinder has given a very scant attention in the literature. Here we have presented an analytical solution of unsteady natural convective flow past an infinite moving vertical cylinder with constant temperature. To solve the governing boundary layer equations, first they are converted into non-dimensional form and then solved by Laplace transform technique.

***Corresponding author: A. Paul*, *E-mail: ashpaul85@gmail.com**

Department of Mathematics, Gauhati University, Guwahati-781014 (India)

2. MATHEMATICAL ANALYSIS:

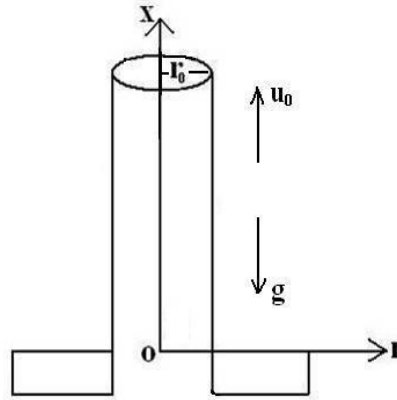


Fig.1: The physical model and co-ordinate system

Consider unsteady, laminar and incompressible viscous flow past an infinite moving vertical cylinder of radius r_0 with constant temperature. The physical model of the problem is shown in Fig 1. Here the x-axis is taken vertically upward along the axis of the cylinder and the radial co-ordinate r is taken normal to the cylinder. Initially it is assumed that the cylinder and fluid are at same temperature T'_∞ . It is also assumed that at $t' \geq 0$, the cylinder starts to move in the vertical direction with constant velocity u_0 and the temperature of the cylinder raised to T'_w . Under these assumptions the governing boundary layer equations for momentum and energy for free convective flow with Boussinesq's approximation are as follows:

$$\frac{\partial u}{\partial t'} = g\beta(T' - T'_\infty) + \frac{\nu}{r} \frac{\partial}{\partial r} \left(r \frac{\partial u}{\partial r} \right) \quad (1)$$

$$\frac{\partial T'}{\partial t'} = \frac{\alpha}{r} \frac{\partial}{\partial r} \left(r \frac{\partial T'}{\partial r} \right) \quad (2)$$

with initial and boundary conditions,

$$\left. \begin{aligned} t' \leq 0: \quad & u = 0, \quad T' = T'_\infty \quad \forall r \\ t' > 0: \quad & u = u_0, \quad T' = T'_w \quad \text{at} \quad r = r_0 \\ & u \rightarrow 0, \quad T' \rightarrow T'_\infty \quad \text{as} \quad r \rightarrow \infty \end{aligned} \right\} \quad (3)$$

Introducing the non dimensional variables

$$\left. \begin{aligned} R = \frac{r}{r_0}, \quad U = \frac{u}{u_0}, \quad t = \frac{t' \nu}{r_0^2}, \quad T = \frac{T' - T'_\infty}{T'_w - T'_\infty} \\ \text{Pr} = \frac{\nu}{\alpha}, \quad Gr = g\beta r_0^2 \frac{T'_w - T'_\infty}{u_0 \nu} \end{aligned} \right\} \quad (4)$$

the equations (1) and (2) reduce to

$$\frac{\partial U}{\partial t} = \frac{\partial^2 U}{\partial R^2} + \frac{1}{R} \frac{\partial U}{\partial R} + GrT \quad (5)$$

$$\frac{\partial T}{\partial t} = \frac{1}{\text{Pr}} \left(\frac{\partial^2 T}{\partial R^2} + \frac{1}{R} \frac{\partial T}{\partial R} \right) \quad (6)$$

with the initial and boundary conditions as:

$$\left. \begin{aligned} t \leq 0: \quad U &= 0, \quad T = 0 \quad \forall R \\ t > 0: \quad U &= 1, \quad T = 1 \quad \text{at } R = 1 \\ U &\rightarrow 0, \quad T \rightarrow 0 \quad \text{as } R \rightarrow \infty \end{aligned} \right\} \quad (7)$$

3. SOLUTION PROCEDURE:

To solve the governing unsteady non dimensional boundary layer equations (5) and (6) subject to initial and boundary conditions (7), we apply the Laplace transform technique.

Laplace transformation of equations (5) and (6) gives

$$\frac{d^2 \bar{U}}{dR^2} + \frac{1}{R} \frac{d\bar{U}}{dR} - p\bar{U} + Gr\bar{T} = 0 \quad (8)$$

$$\frac{d^2 \bar{T}}{dR^2} + \frac{1}{R} \frac{d\bar{T}}{dR} - pPr\bar{T} = 0 \quad (9)$$

where p is the of Laplace transform parameter defined by $L\{f(t)\} = F(p)$, L being the Laplace operator and \bar{U} and \bar{T} are Laplace transform of U and T respectively.

Solution of the equation (9) subject to initial and boundary conditions (7) gives

$$\bar{T} = \frac{K_0(R\sqrt{pPr})}{pK_0(\sqrt{pPr})} \quad (10)$$

Using the equation (10) with initial and boundary conditions (7), we obtain the solution of the equation (8) as:

$$\bar{U} = \frac{K_0(R\sqrt{p})}{pK_0(\sqrt{p})} + \frac{Gr}{2p\sqrt{p}} \left\{ R \frac{K_1(R\sqrt{p})}{K_0(\sqrt{p})} - \frac{K_1(\sqrt{p})K_0(R\sqrt{p})}{K_0^2(\sqrt{p})} \right\} \quad (\text{for } Pr = 1) \quad (11)$$

and

$$\bar{U} = \frac{K_0(R\sqrt{p})}{pK_0(\sqrt{p})} + \frac{Gr}{p^2(1-Pr)} \left\{ \frac{K_0(R\sqrt{pPr})}{K_0(\sqrt{pPr})} - \frac{K_0(R\sqrt{p})}{K_0(\sqrt{p})} \right\} \quad (\text{for } Pr \neq 1) \quad (12)$$

Now, using the theorem of inverse Laplace transform in equation (10), we have

$$T = \frac{1}{2\pi i} \int_{\gamma-i\infty}^{\gamma+i\infty} e^{pt} \frac{K_0(R\sqrt{pPr})}{pK_0(\sqrt{pPr})} dp \quad (13)$$

The integrand of (13) has a branch point at $p = 0$ and a simple pole at $p = 0$

Now $K_0(\sqrt{pPr})$ do not have zero at any point in the real and imaginary plane if the branch cut is made along the negative real axis. To obtain $T(t, R)$ from $\bar{T}(p, R)$, we use the adjoining contour Fig.2. Therefore the line integral in (13) may be replaced by the limit of the sum of the integrals over FE, ED, DC, CB, and BA as $S_1 \rightarrow \infty$ and $S_0 \rightarrow 0$.

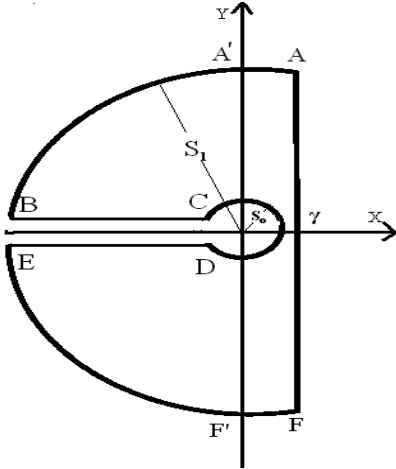


Fig.2: path of contour integration for the inverse integral.

The particular form of the inversion integral, equation (13) has chosen because the value along the paths DC, BA and FE approaches zero as $S_1 \rightarrow \infty$ and $S_0 \rightarrow 0$.

Along the path CB and ED we choose $p = \frac{V^2}{\text{Pr}} e^{i\pi}$ and $p = \frac{V^2}{\text{Pr}} e^{-i\pi}$ respectively.

\therefore on the path CB

$$T_{CB} = \frac{1}{\pi i} \int_0^\infty e^{-\frac{V^2}{\text{Pr}} t} \frac{J_0(RV) - iY_0(RV)}{V\{J_0(V) - iY_0(V)\}} dV \quad (14)$$

and on the path ED

$$T_{ED} = \frac{1}{\pi i} \int_0^\infty e^{-\frac{V^2}{\text{Pr}} t} \frac{J_0(RV) + iY_0(RV)}{V\{J_0(V) + iY_0(V)\}} dV \quad (15)$$

The sum of the integral along CB and ED gives

$$T_{CB+ED} = \frac{2}{\pi} \int_0^\infty e^{-\frac{V^2}{\text{Pr}} t} \frac{J_0(RV)Y_0(V) - Y_0(RV)J_0(V)}{V\{J_0^2(V) + Y_0^2(V)\}} dV \quad (16)$$

Also, the residue of the integrand of (13) at the point $p = 0$ is =1

Thus from the theory of residues we have

$$T = 1 + \frac{2}{\pi} \int_0^\infty e^{-\frac{V^2}{\text{Pr}} t} \Gamma(R, V) \frac{dV}{V} \quad (17)$$

$$\text{Where } \Gamma(R, V) = \frac{J_0(RV)Y_0(V) - Y_0(RV)J_0(V)}{J_0^2(V) + Y_0^2(V)} \quad (18)$$

Similarly we obtained the inverse Laplace transforms of equations (11) and (12), which gives the expression of velocity profiles for $\text{Pr} = 1$ and for $\text{Pr} \neq 1$ respectively as:

$$U = 1 + \frac{2}{\pi} \int_0^\infty e^{-V^2 t} \Gamma(R, V) \frac{dV}{V} + \frac{Gr}{\pi} \int_0^\infty \left(1 - e^{-V^2 t}\right) \left[R \frac{J_1(RV)Y_0(V) - Y_1(RV)J_0(V)}{J_0^2(V) + Y_0^2(V)} + \frac{\{Y_1(V)J_0(RV) + Y_0(RV)J_1(V)\} \{J_0^2(V) - Y_0^2(V)\}}{\{J_0^2(V) + Y_0^2(V)\}^2} - \frac{2J_0(V)Y_0(V) \{J_1(V)J_0(RV) - Y_1(V)Y_0(RV)\}}{\{J_0^2(V) + Y_0^2(V)\}^2} \right] \frac{dV}{V^2}$$

(for $Pr = 1$) (19)

and

$$U = 1 + \frac{2}{\pi} \int_0^\infty e^{-V^2 t} \Gamma(R, V) \frac{dV}{V} + \frac{2GrPr}{(Pr-1)\pi} \int_0^\infty \left(1 - e^{-\frac{V^2}{Pr}t}\right) \left\{ \Gamma\left(R, \frac{V}{\sqrt{Pr}}\right) - \Gamma(R, V) \right\} \frac{dV}{V^3} \quad (\text{for } Pr \neq 1) \quad (20)$$

3.1 skin friction:

Non-dimensional skin friction $\tau = -\frac{\partial U}{\partial R} \Big|_{R=1}$ obtained from equation (19) and (20) for $Pr = 1$ and $Pr \neq 1$ respectively as:

$$\tau = \frac{2}{\pi} \int_0^\infty e^{-V^2 t} \Gamma(V) dV + \frac{Gr}{\pi} \int_0^\infty \left(1 - e^{-V^2 t}\right) \left[-\frac{2\{J_1(V)Y_0(V) - Y_1(V)J_0(V)\} + V\{J_0(V)Y_2(V) - Y_0(V)J_2(V)\}}{2\{J_0^2(V) + Y_0^2(V)\}} + 2V \frac{J_1(V)Y_1(V) \{J_0^2(V) - Y_0^2(V)\} - Y_0(V)J_0(V) \{J_1^2(V) - Y_1^2(V)\}}{\{J_0^2(V) + Y_0^2(V)\}^2} \right] \frac{dV}{V^2}$$

(21)

and

$$\tau = \frac{2}{\pi} \int_0^\infty e^{-V^2 t} \Gamma(V) dV + \frac{2GrPr}{(Pr-1)\pi} \int_0^\infty \left(1 - e^{-\frac{V^2}{Pr}t}\right) \left\{ \Gamma_1\left(\frac{V}{\sqrt{Pr}}\right) / \sqrt{Pr} - \Gamma_1(V) \right\} \frac{dV}{V^2} \quad (22)$$

3.2 nusselt number:

Non-dimensional Nusselt number $Nu = -\frac{\partial T}{\partial R} \Big|_{R=1}$ obtained from equation (10) as:

$$Nu = \frac{2}{\pi} \int_0^\infty e^{-\frac{V^2}{Pr}t} \Gamma_1(V) dV \quad (23)$$

where

$$\Gamma_1(V) = \frac{J_1(V)Y_0(V) - Y_1(V)J_0(V)}{J_0^2(V) + Y_0^2(V)} \quad (14)$$

4. RESULTS AND DISCUSSIONS:

In order to understand the effects of different physical parameters in the flow problem, the velocity profiles, temperature profiles, skin-friction and Nusselt number have been discussed by assigning numerical values to various parameters, namely Grashof number, Prandtl number and time. Since water and air are the most commonly occurring fluids in nature, we basically restricted our observations for $Pr=0.71$ (air) and $Pr=7$ (water).

Fig.3 shows the velocity profile against radial distance R at $t=0.6$. It exhibits the effects of Grashof number Gr and Prandtl number Pr . It is observed that an increase in Gr , leads to an increase in velocity. It is because increasing Gr gives rise to buoyancy effects resulting in more induced flows. Magnitude of velocity for air is greater than water. Physically, this is possible because fluids with high Prandtl number have high viscosity hence move slowly. Fig.4 shows the effect of t at $Gr=5$ and $Pr=0.71$. It is observed from the figure that velocity rises rapidly with increasing time t .

The transient temperature profiles against radial distance R for different Pr and t are plotted on Fig.5. It is observed that the magnitude of temperature is maximum at the surface of the cylinder and decay to zero asymptotically. Temperature increases with increased values of t or decrease values of Prandtl number. Fig.6 shows temperature profiles against time. It is clear from the figure that initially temperature increases sharply with time and at larger time it becomes steady. Also time require to reach the steady state increases with increase in Pr .

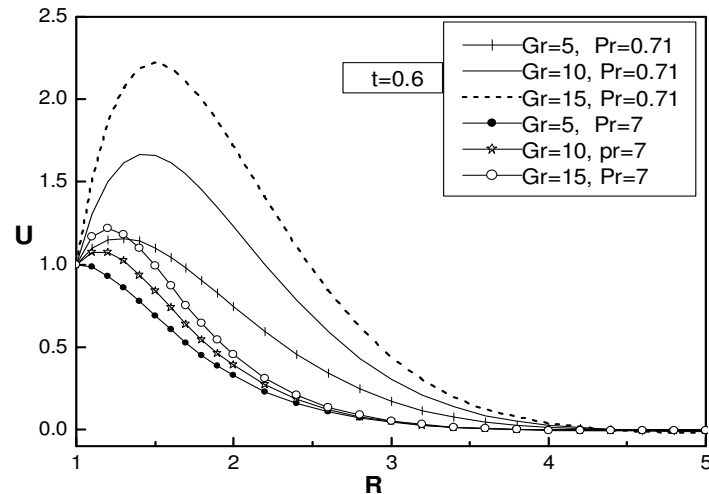


Fig.3: Effects of Gr & Pr on velocity profiles at $t=0.6$

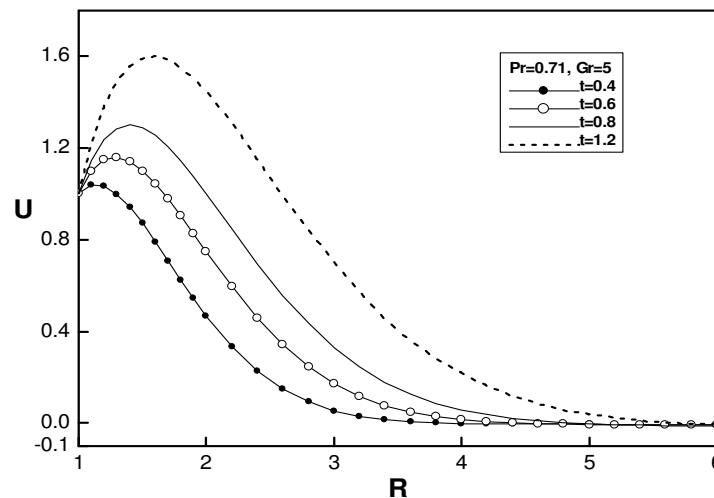


Fig.4: Velocity profiles for various times at $Pr=0.71$, $Gr=5$

Fig.7 exhibits the skin friction against time for different values of Grashof number Gr and Prandtl number $Pr=0.71$ & 7 . The results show that an increase of Gr , decreases the skin friction for both air and water. Also skin friction increases with increase in Prandtl number.

Fig.8 shows the effect of Prandtl number on Nusselt number against time. It is observed that rate of heat transfer i.e. Nusselt number increases with increase in Pr .

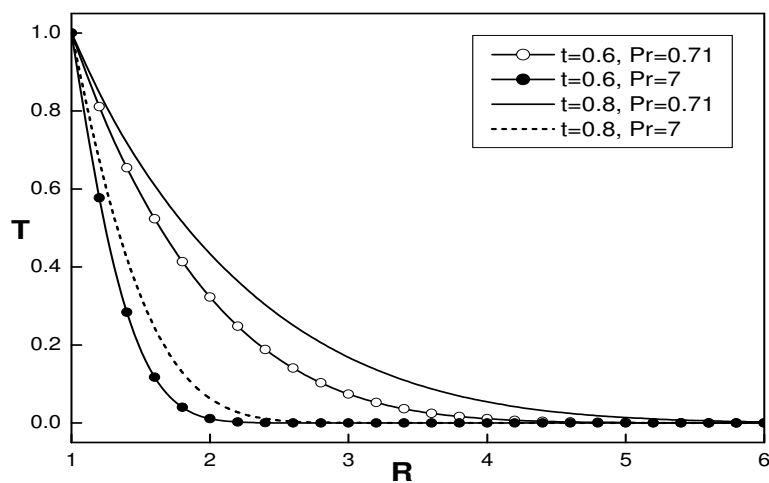


Fig.5: Effects of Pr and t on temperature profiles.

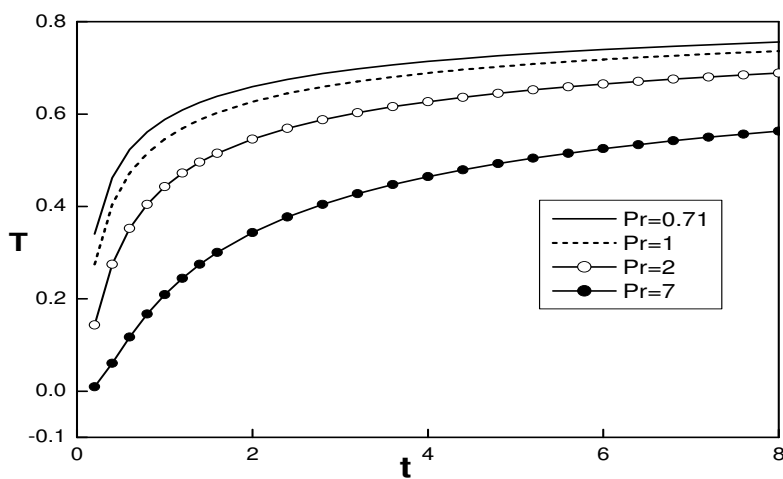


Fig.6: Temperature profiles with respect to time for different values of Pr.

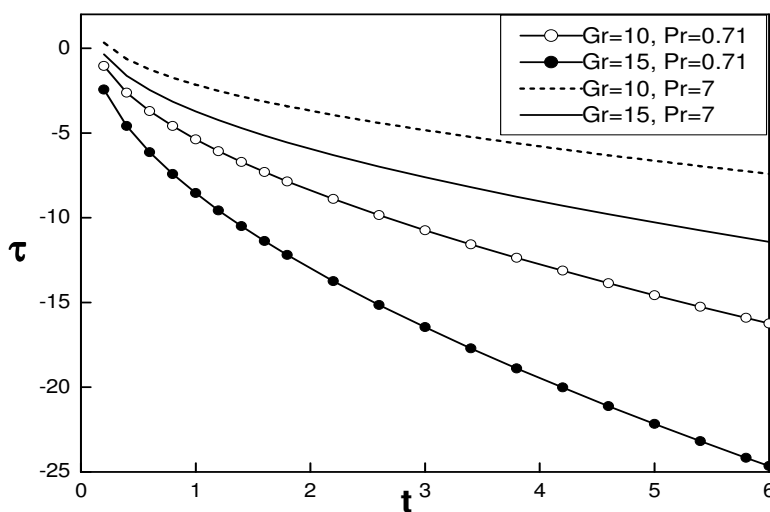


Fig.7: Effects of Gr and Pr on Skin friction.

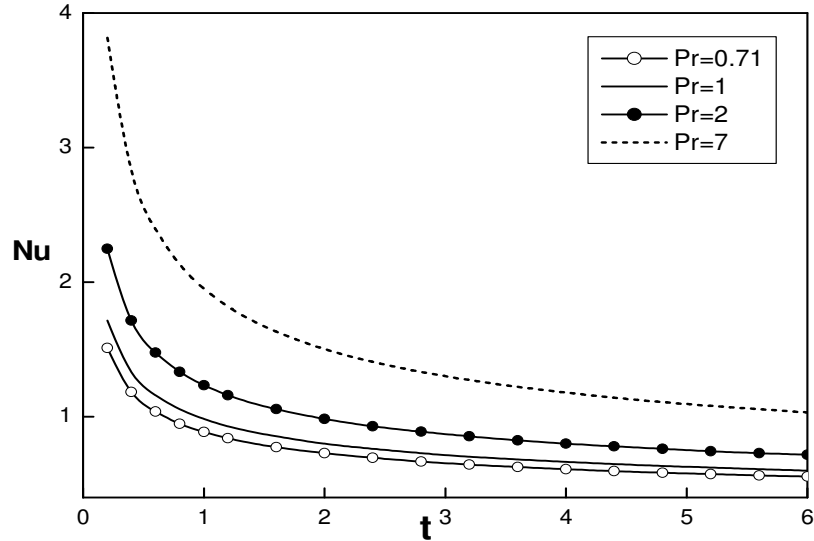


Fig.8: Effect of Prandtl number on Nusselt number.

Thus on the basis of the results obtained from the above discussions we conclude as follows:

- (i) Velocity increases with increase of Gr or t but decreases as Pr increases.
- (ii) Temperature increases with increase in t but decreases with increase in Pr . Initially temperature increases sharply with time and at larger time it becomes steady
- (iii) Skin friction decreases with increase in Gr and increases with increase in Pr .
- (iv) Nusselt number increases as Pr increases. Also, Nusselt number decreases initially but after certain time it approaches a fixed value.

NOMENCLATURE:

Gr	Grashof number	T'	temperature
g	acceleration due to gravity	T	dimensionless temperature
J_0	Bessel function of first kind and order zero	u	x -component of velocity
J_1	Bessel function of first kind and order one	u_0	vertical velocity of the cylinder
Nu	Nusselt number	U	dimensionless velocity
Pr	Prandtl number of fluid	V	dummy real variable used in inverse transform of loop integral
r	radial coordinate measured from the axis of the cylinder	Y_0	Bessel function of second kind and order zero
r_0	radius of the cylinder	Y_1	Bessel function of second kind and order one
R	dimensionless radial coordinate	α	Thermal diffusivity of fluid
t'	time	β	coefficient of thermal expansion of fluid
t	dimensionless time	ν	kinematic viscosity

REFERENCE:

- [1] Bottemanne G. A. Experimental results of pure and simultaneous heat and mass transfer by free convection about a vertical cylinder for $Pr=0.71$ and $Sc=0.63$. Appl Sci Res (1972), 25, 372–382.
- [2] Carslaw H. S., Jaeger J. C. Operational methods in Applied Mathematics, Second edition, Oxford Press., (1948).
- [3] Carslaw H. S., Jaeger J. C. Conduction of heat in solids, Second edition, Oxford Press. (1959).
- [4] Chen T.S., Yuh C.F. Combined heat and mass transfer in natural convection along a vertical cylinder. Int J Heat Mass Trans (1980), 23, 451–461.

- [5] Elgazery, Nasser S., Hassan, M.A. Numerical study of radiation effect on MHD transient mixed-convection flow over a moving vertical cylinder with constant heat flux. Communications in Numerical Methods in Engineering (2008), 24(11), 1183–1202.
- [6] Ganesan, P., Rani, H.P. Transient natural convection along vertical cylinder with Heat and Mass transfer. Heat Mass Transfer. (1998), 33, 449–456.
- [7] Ganesan, P., Loganathan, P. Effects of mass transfer and flow past a moving vertical cylinder with constant heat flux. Acta Machanica. (2001), 150, 179-190.
- [8] Ganesan, P., Loganathan, P. Unsteady natural convective flow past a moving vertical cylinder with heat and mass transfer. Heat Mass Transfer. (2001), 37, 59–65.
- [9] Ganesan, P., Loganathan, P. Numerical study of double-diffusive, free convective flow past moving vertical cylinder with chemically reactive species diffusion, J. Eng. Phys. Thermophys., (2006), 79, 73–78.
- [10] Gebhart, B., Pera, L. The nature of vertical natural convection flows resulting from the combined buoyancy effects of thermal and mass diffusion, Int. J. Heat Mass Transfer, 14, 2025–2050, (1971).
- [11] Goldstein, R. J., Briggs, D. G. Transient free convection about a vertical plates and circular cylinders. Trans ASME C: J. Heat Transfer (1964), 86, 490-500.
- [12] Nagendra, H. R., Tirunarayanan, M. A., Ramachandran, A. Laminar Free Convection From Vertical Cylinders With Uniform Heat Flux, J. Heat Transfer (1970), 92(1), 191-194.
- [13] Reddy, M. M. G., Reddy, N. B. Radiation and mass transfer effects on unsteady MHD free convection flow of an incompressible viscous fluid past a moving vertical cylinder. Theoretical applied Mechanics (2009), 36(3), 239-260.
- [14] Reddy, M. M. G., Reddy, N. B. Thermal radiation and mass transfer effects on MHD free convection flow past a vertical cylinder with variable surface temperature and concentration. Journal of Naval Architecture and Marine Engineering (2009), 6(1), 1-24.
- [15] Sparrow, E. M., Gregg, J. L. Laminar free convection heat transfer from the outer surface of a vertical circular cylinder. Trans. ASME. (1956), 78, 1823-1829.
